Measurement of the Z Production Cross Section, Mass, and Width in pp Collisions

Ian P. Haines[1, *]

[1]*Department of Physics, University of California, Berkeley, CA 94720-3411, USA*

(Dated: August 22, 2021)

We analyze dimuon decay data from the CMS Collaboration at the LHC at CERN. The muon decays were collected at the CMS Detector at the LHC with a corresponding integrated luminosity 2.1 fb^{-1}. The measured inclusive cross section is $\sigma(pp \to ZX) = \pm err$ pb. when we restrict our attention to the dimuon invariant mass range of 60 to 120 GeV. We also find a mass of $m_Z = 91.25 \pm err$ GeV and a width of $\Gamma_Z = 2.53 \pm err$ GeV. Although these results are not within the current precision error ranges, they are within a reasonable error according to accepted values [**?**] [**?**]

I. INTRODUCTION

The Z boson is of fundamental importance to the Standard Model and its discovery was one of the crowning achievements of not only experimental particle physics but theoretical particle physics as well via the justification of the unified electroweak theory as proposed by Glashow, Salam, and Weinberg. Precise determinations of the properties of the Z boson allows us to refine our current models of particle physics and subsequently search for beyond Standard Model physics.

Z bosons are primarily produced in the electroweak Drell-Yan (DY) process [**?**]. Production of Z bosons via DY is studied extensively at the LHC. In the parton model, DY occurs when one parton scatters inelastically off of another parton. At energies such as those attained at the LHC, Z boson production occurs. To measure the properties of the Z boson, proper measurements of the kinematic quantities must first be obtained. The mass and rapidity, m_Z and y, can be calculated from the momentum fractions of the colliding partons via the relations $m_Z^2 = sx_1x_2$ and $y = 1/2 \ln x_1/x_2$. Decays via $Z \to \ell^+\ell^-$ are observed at the CMS detector and measurements of the kinematic variables of the dilepton pairs can be obtained thus giving us a way to calculate Z properties.

The paper is organized as follows: we first give an overview of how the CMS detector operates. The succeeding section describes the data sample used in our analysis. Next, we discuss our analysis of the data and the subsequent results. Afterwards, we discuss any possible errors and uncertainties in our calculations. Finally, we give some concluding thoughts and future considerations.

*ianphaines@berkeley.edu

II. THE CMS DETECTOR

The CMS Detector at the LHC is composed of layers of silicon trackers and silicon strips. These detect hits from charged particles which are then used to reconstruct tracks. These trackers and strips rest inside an electromagnetic calorimeter (ECAL) which consists of lead tungstate crystals. The ECAL rests inside a hadron calorimeter (HCAL) which consists of brass and a plastic scintillator. Covering the HCAL is a superconducting solenoid which is 6m in its internal diameter. The outer layers consist of a steel yoke which has alternating layers of muon drift chambers that capture the muons for recording purposes. On the outer ends perpendicular to the axis running through the solenoid are the endcaps which also have drift chambers in them to detect particles [**?**].

For the CMS detector, we use a right-handed coordinate system with the positive z-axis pointing in the direction of the axis through the center of the solenoid and anticlockwise to the direction of the beam. The scattering angle, θ, lies in the xz-plane and is measured from the positive z-axis. The azimuthal angle, ϕ, is measured from the xy-plane. We measure the pseudorapidity, η, via the relation $\eta = -\ln\tan(\theta/2)$.

Muons are detected with a pseudorapidity value $|\eta| < 2.4$ via detection planes that use drift tubes, cathode strip chambers, and resistive plate chambers. Muons with high transverse momenta, p_T, produce tracks in muon stations. These tracks are then matched with the inner tracks picked up by the silicon detectors. The CMS Detector works via a trigger system, with the first level trigger being offline and hardware based and a high-level trigger (HLT) being online and software based. A proper trigger system allows for rapid detection of good candidate muons for analysis. More information regarding the construction of these tracks and the CMS detector can be found in [**?**][**?**].

III. CMS DATA

The CMS collaboration consists of more than 3,000 scientists, engineers, and professionals around the world. The purpose of this collaboration is to expand the knowledge of fundamental physics and provide data for others to use. The data used in this analysis was collected during the LHC data operations during 2011. This data can be found on the CERN open data web page resource. CERN provides open data for others at no charge for analysis and educational purposes. The data used in our analysis is purely for educational purposes and is not of the quality for proper analysis to obtain publishable results [**?**].

In our dataset, the acceptance rate is 40%, the muon efficiency rate is 90%, and the integrated luminosity is 2.1pb^{-1}. The muon candidates satisfied strict criteria as detailed and further explained in [**?**]. Both candidates in an event had to have $p_T > 20$ GeV, $|\eta| < 2.1$, and $60 < M_{\mu\mu} < 120$ GeV. These requirements refined the original dataset from 450,000+ decay events down to 10,582 acceptable decay events from which an analysis was performed. As a result, we were able to determine the key properties of the Z from the refined dataset.

IV. ANALYSIS AND RESULTS

Our analysis is as follows: we first calculated the invariant mass of the muons to determine where the mass was peaked around since this should give us the approximate Z mass resonance (fig 1). We used the formula:

$$M_{\mu\mu}^2 = 2p_{T_1}p_{T_2}[\cosh(\eta_1 - \eta_2) - \cos(\phi_1 - \phi_2)] \quad (1)$$

On inspection, we noticed a strong background noise on the lower end of the mass spectrum. Specifically, we noticed that there appeared to be some leftover excess noise from the initial cut applied to the dataset. In the original data, the frequency of mass values less than 60 increases as one decreases the mass. This is due to the fact that the cross section decreases as the dimuon mass increases for $M_{\mu\mu} < 80$ GeV. From the range 80 GeV $< M_{\mu\mu} <$ 100 GeV. Finally, for $M_{\mu\mu} > 100$ GeV, we see a decrease again. As a result, we first focused on a window (IW) such that the noise was minimized and we could focus on the signal to determine the mass of the Z (fig 2). This allowed us to determine sidebands (SB) with lower sidebands (LSB) and higher sidebands (HSB) from which we could compare the IW signal and noise and the SB signal and noise (figs 3-8).

We tried multiple fits to the data to determine the signal. We first attempted just a Crystal Ball [**?**] fit with various parameters (fig 9), where the Crystal Ball is a gaussian core that decreases like a power law on the

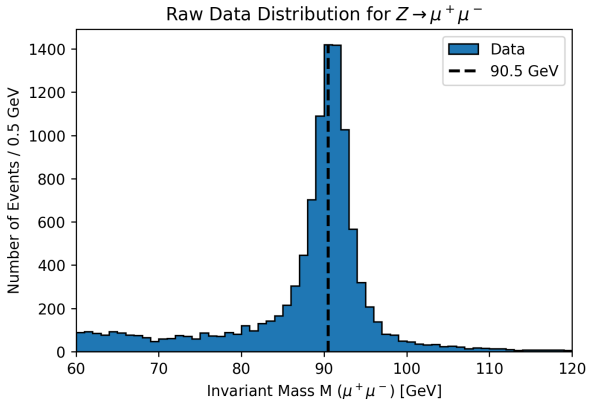

FIG. 1: Distribution of the invariant dimuon mass over 60 equally sized bins for all events that passed the initial filtering criteria. Before any analysis was done, the calculated mass of the Z is only $\sim 0.75\%$ different from the accepted value of $m_Z = 91.1876 \pm 0.0021$ GeV [**?**]

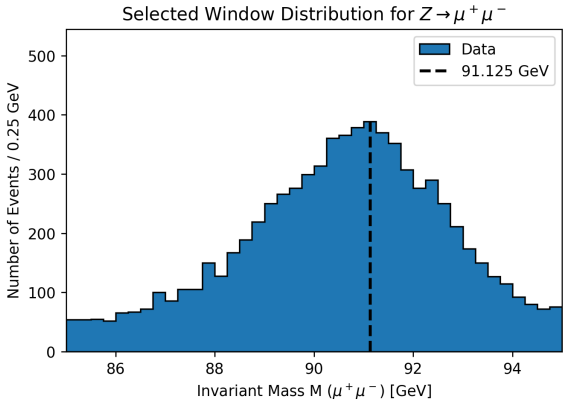

FIG. 2: IW of the mass spectrum that determines m_Z more accurately than the entire mass spectrum.

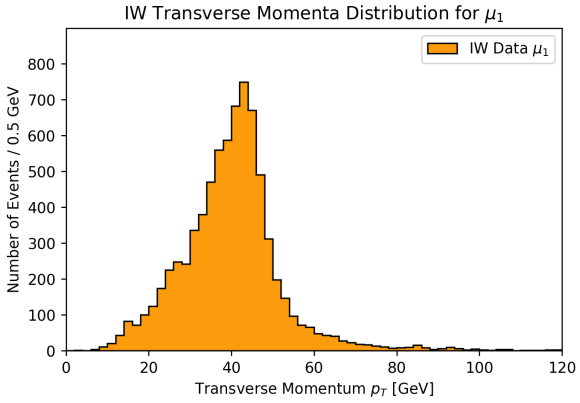

FIG. 3: IW transverse momenta for μ^1. We can see that the frequency increases at an increasing rate until it reaches a peak at around ~ 41 GeV and drops dramatically after that.

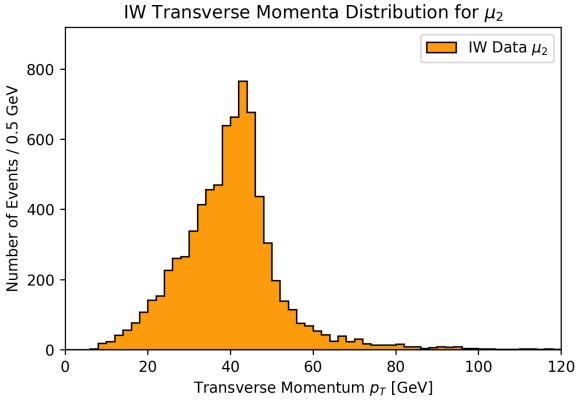

FIG. 4: IW transverse momenta for μ^2. Refer to fig 2 for an explanation.

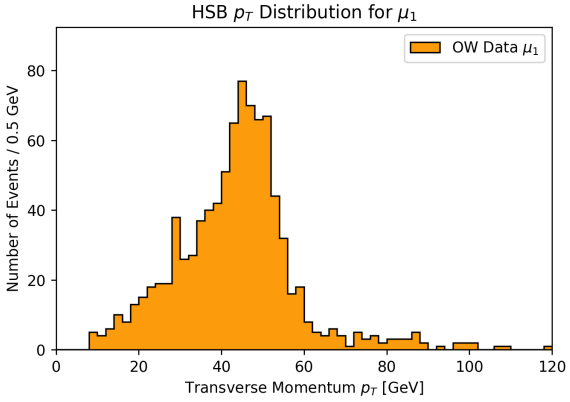

FIG. 7: HSB transverse momenta for μ^1. We can see that the frequency increases at an increasing rate with a peak that is ~ 45 GeV and drops off but not as dramatically as we saw for IW p_T.

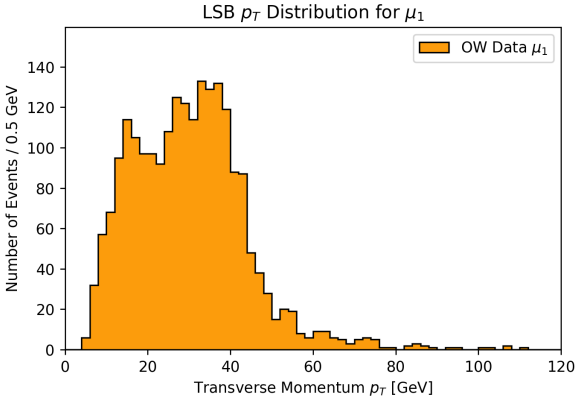

FIG. 5: LSB transverse momenta for μ^1. We can see that the frequency increases at a roughly decreasing rate with a greater frequency for lower values.

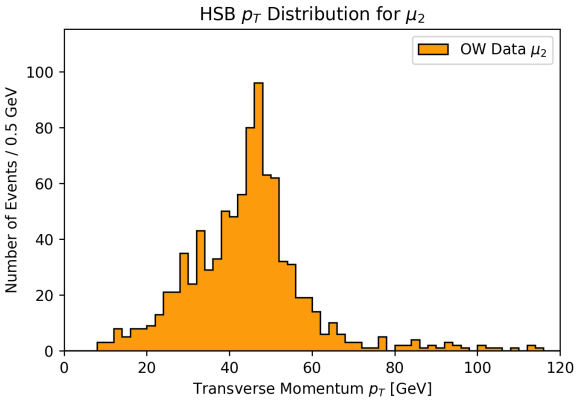

FIG. 8: HSB transverse momenta for μ^2. We can see that the frequency increases at an increasing rate with a peak that is ~ 45 GeV and drops off but not as dramatically as we saw for IW p_T.

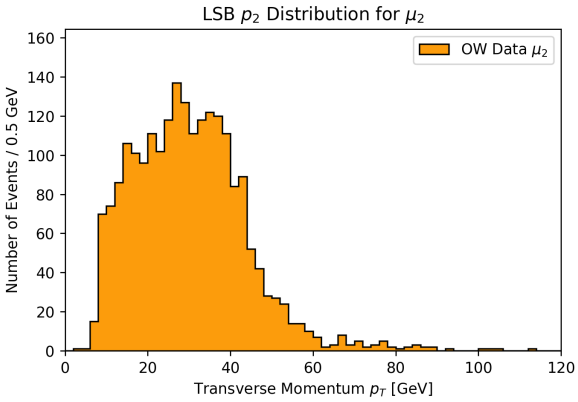

FIG. 6: LSB transverse momenta for μ^2. We can see that the frequency increases at a roughly decreasing rate with a greater frequency for lower values.

tails:

$$f(x;\alpha,n,\bar{x},\sigma) = N\cdot\begin{cases}\exp(-\frac{(x-\bar{x})^2}{2\sigma^2}), & \text{for } \frac{x-\bar{x}}{\sigma} > -\alpha \\ A\cdot(B-\frac{x-\bar{x}}{\sigma})^{-n}, & \text{for } \frac{x-\bar{x}}{\sigma} - \alpha\end{cases} \tag{2}$$

where

$$A = \left(\frac{n}{|\alpha|}\right)^n \cdot \exp\left(-\frac{|\alpha|^2}{2}\right) \tag{3}$$

and

$$B = \frac{n}{|\alpha|} - |\alpha| \tag{4}$$

Then we tried a Breit-Wigner distribution fit (fig 10):

$$f(E;M,\Gamma) = \frac{k}{(E^2-M^2)^2 + M^2\Gamma^2} \tag{5}$$

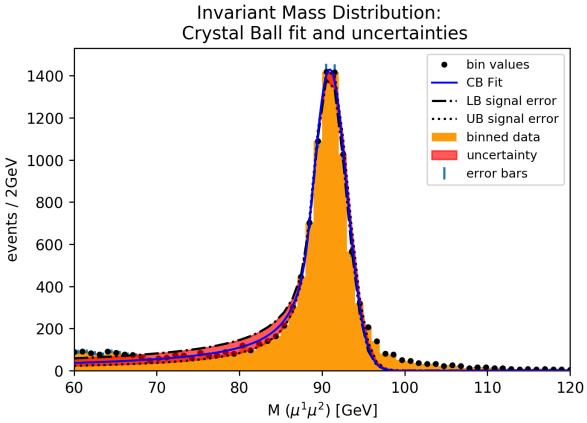

FIG. 9: Crystal Ball function fit to data. We added a range of uncertainties as given by the square root of the diagonal of the covariance matrix generated from performing a least squares fit. We notice that the uncertainties are greatest for masses lower than m_Z.

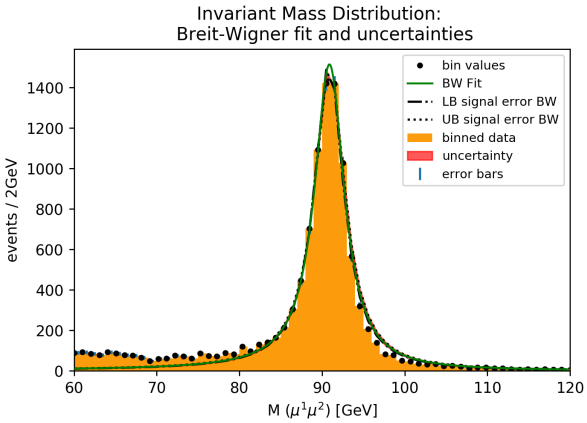

FIG. 10: Breit-Wigner distribution fit to data. We added a range of uncertainties as given by the square root of the diagonal of the covariance matrix generated from performing a least squares fit. We notice that the uncertainties are minimized despite the fit not fitting the data well for ranges beyond a few GeV from m_Z

where

$$k = \frac{2\sqrt{2}M\Gamma\gamma}{\pi\sqrt{M^2+\gamma}} \tag{6}$$

and

$$\gamma = \sqrt{M^2\left(M^2+\Gamma^2\right)}. \tag{7}$$

Finally, we tried a Breit-Wigner convolved with a Crystal Ball with the Crystal Ball being fitted to the data for $M_{\mu\mu} \leq m_Z$ and the Breit-Wigner being fit to the data for $M_{\mu\mu} > m_Z$ (fig 11)

We determined after choosing our fit and removing the

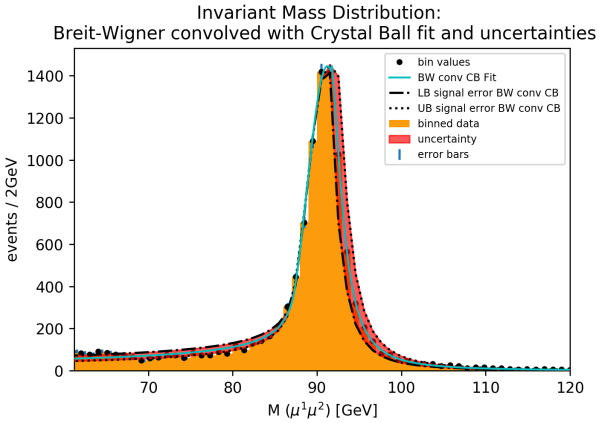

FIG. 11: Breit-Wigner convolved with a Crystal Ball to accurately fit both the tails of the mass spectrum. We see that for higher values that the rate of decrease in the frequency is greater than that on the left. The convolved function allows for a gaussian core with a power law tail.

systematic noise for the lower mass spectrum that the noise in the range $M > 80$ GeV was random as can be see how our residuals display no perference for positive or negative values and are spread out randomly (fig 14). Thus, we chose to fit an exponential to the systematic background noise in the lower mass range. Our reasoning is as follows: we will see an overlap between good dimuons and the lower quality dimuon events that we originally removed from initial requirements that $60 < M < 120$ GeV, $|\eta| < 2.1$, and $p_T > 20$ GeV. Although these dimuon pairs satisfy our strict requirements, they are more likely to have a mass in the 50 GeV $< M <$ 70 GeV than in the range 70 GeV $< M <$ 80 GeV. As a result, this creates a greater random noise that sits on top of our signal for the lower mass range we perform our analysis upon. So, we took our Crystal Ball fit and used that as the signal model for the range we wanted to remove the noise from. This attempts to capture the random noise we see from the dimuon candidates (fig 12).

With the noise removed, we could then get a more accurate fit to the signal with the convolved function (fig 13). After performing this fit, we calculated the residuals to see whether or not there was a systematic error in our fit (fig 14), and we determined that because of the lack of preference for either mostly positive or mostly negative residual values that our fit did not suffer from any systematic uncertainties. We were still unable to remove some of the random noise in the data that we used. We note that we did not want to use a filter on the fit in the event that the filter would introduce an artificial element into the relation between the mass and the frequency. This overfitting could potentially skew our calculated values for σ, m_Z and Γ. Moreover, we performed a reduced χ^2 goodness-of-fit test. We found

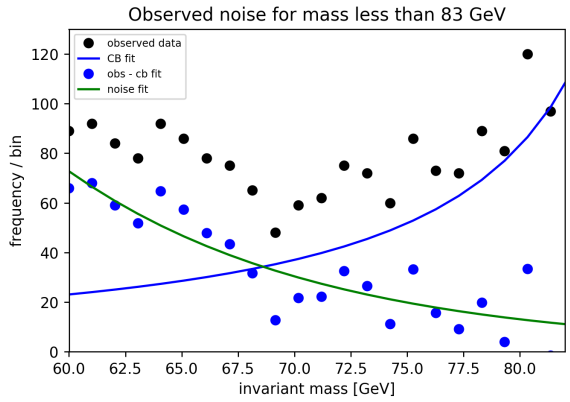

FIG. 12: Exponential fit to the random noise we see. We can see that although the noise is random is does have an exponential decay pattern to it.

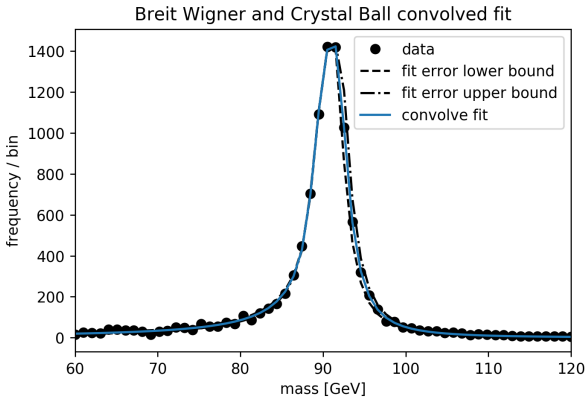

FIG. 13: Convolved Breit-Wigner and Crystal Ball fit to the new data which shows less noise and a true signal for the lower mass range.

that using 8 parameters, 3 for the Breit-Wigner and 5 for the Crystal Ball, gave us 52 degrees of freedom and thus a reduced χ^2 value of 1.66. Moreover, this gives us a p-value of 0.001786 which indicates that our hypothesis for the signal and subsequent fit is good.

Once we determined our fit we were able to use our fit parameters to determine the mass, width, and cross section of the Z. For the cross section, we used the formula

$$\sigma = \frac{(S-B)}{(A \times E \times L)} \tag{8}$$

where S is the signal, B is the background, A is the acceptance, E is the efficiency, and L is the luminosity. We had 10,582 total events initially. After fitting our background, we found that our number of signal events was approximately 9,767 $\pm$ 321 events while the number of background events was approximately 817 $\pm$ 391 events. Using these values we calculate $\sigma = 12919$ fb$\pm$431.2 fb. For the mass, we took an average of the fit mass used for

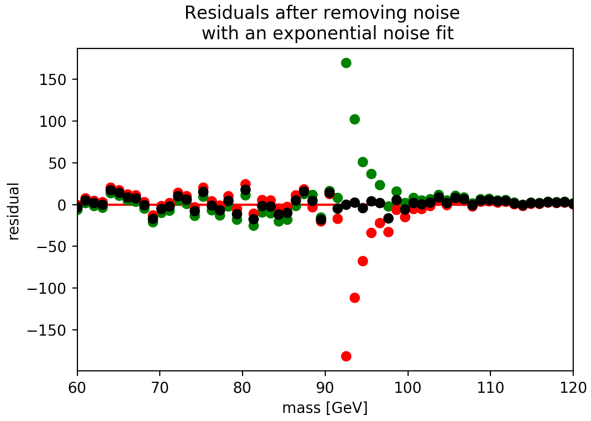

FIG. 14: Calculated residuals between fit and the frequency values of the mass spectra

the Breit-Wigner and Crystal-Ball fits. For the width, we did the same procedure. Our values obtained from our fits are given in Table below.

Fit	m_Z	Γ_Z
CB	91.378 $\pm$ 0.1628	3.3914 $\pm$ 0.0755
BW	91.071 $\pm$ 0.0354	2.1434 $\pm$ 0.03862

These give us a mass of $m_Z = 91.2245$ GeV and width $\Gamma_Z = 2.7674$ GeV.

V. CONCLUSION

Knowing the key properties of the Z boson are of vital importance for testing the Standard Model and Beyond Standard Model physics. In this paper we have analyzed a dataset of dimuon pairs produced in the decay of Z bosons taken from the CMS open data website. This data is for purely educational purposes in nature and therefore does not constitute the same quality data as would be seen in a published paper. However, this data, with the proper analysis, can give insight into the properties of the Z. In analyzing this data we have determined that with an integrated luminosity of 2.1 fb^{-1} that the production cross section is 12919 $\pm$ 431.2 fb, the mass is $m_Z = 91.2245$ GeV and the decay width is $\Gamma_Z = 2.7674$ GeV. These values are not quite up to par with currently accepted values [**?**], especially our width value which is more than 8% inaccurate.

VI. ACKNOWLEDGEMENTS

I would like to thank Professor Marjorie Shapiro for her masterful ability to teach and present the fundamental aspects of particle physics. Such an ability has ignited within me a passion for high energy physics and I have been exceptionally grateful to have been a part of her class during this time.